Chemical Geology 390 (2014) 164–172

Contents lists available at ScienceDirect

Chemical Geology

journal homepage: www.elsevier.com/locate/chemgeo

# Selenium isotopes trace anoxic and ferruginous seawater conditions in the Early Cambrian

Hanjie Wen [a,*], Jean Carignan [b], Xuelei Chu [c], Haifeng Fan [a], Christophe Cloquet [d], Jing Huang [e], Yuxu Zhang [a], Huajin Chang [c]

[a] State Key Laboratory of Ore Deposit Geochemistry (SKLODG), Institute of Geochemistry, Chinese Academy of Sciences, Guiyang 550002, China
[b] TAKUVIK, International Center for Arctic and Sub-Arctic Eco-Geosystems Studies, CNRS UMI 3376, Université Laval, Centre d'études Nordiques, Québec, Canada
[c] State Key Laboratory of Lithospheric Evolution, Institute of Geology and Geophysics, Chinese Academy of Science, Beijing 100029, China
[d] Centre de Recherches Petrographique et Geochimiques, CNRS, 15, Rue Notre-Dame-Pauvrves, B. P. 20, 54501, Vandoeuvre-les-Nancy Cedex, France
[e] CAS Key Laboratory of Crust-Mantle Materials and Environments, School of Earth and Space Sciences, University of Science and Technology of China, Hefei 230026, China

ARTICLE INFO

*Article history:*
Received 2 June 2014
Received in revised form 21 September 2014
Accepted 23 October 2014
Available online 29 October 2014

Editor: Michael E. Böttcher

*Keywords:*
Se isotope
Isotopic fractionation
Anoxic and ferruginous sediments
Cambrian
Southern China

ABSTRACT

Selenium (Se) isotopes can yield substantial isotopic fractionation (up to 20‰) confirmed by experiments and field investigations, depending on various biotic or abiotic redox transformations. Therefore, it is expected that redox changes in the ancient oceans would induce significant isotopic fractionation, and the Se isotopic signatures recorded in old sedimentary rocks might provide new insight into how the redox state of the ancient ocean has evolved. However, previous studies have shown that Se is slightly enriched in the lighter isotope relative to the bulk earth values in most deposited conditions (oxic, anoxic, and even sulfidic). Here, our results reveal that ferruginous conditions can result in excessive accumulation of Se in sediments with an elevated Se/S ratio and significant isotope fractionation (about 6‰), which leads us to propose that Se isotopes are an appropriate geochemical proxy to trace unique oceanic conditions over times. Accordingly, Se isotopic variations measured in three Early Cambrian formations in southern China suggest that anoxic waters with ferruginous conditions must have been present in early Cambrian ocean along the eastern margin of the Yangtze platform, and oceanic circulation was stepwise reorganized. This may have triggered biological diversification from the Ediacaran to the Early Cambrian.



## 1. Introduction

Redox-sensitive metals (e.g., Fe, Mo) and their isotopes have been increasingly used as proxies for changing redox conditions in the oceans (Anbar and Rouxel, 2007). Selenium is also redox-sensitive, potentially existing in four redox states (VI, IV, 0 and -II), and its chemical behaviour depends strongly on redox reactions (Johnson, 2004). Under oxidizing conditions, Se(VI) is favored thermodynamically and forms the selenate ($SeO_4^{2-}$) anion, is highly soluble and not strongly adsorbing (Neal and Sposito, 1989); under mild reducing conditions, Se(VI) is reduced to Se(IV) (selenite, $SeO_3^{2-}$ and biselenite, $HSeO_3^-$), is highly soluble and strongly absorbing onto Fe and Al oxides. Under moderate reducing conditions, Se(IV) reduces to Se(0). Under strong reducing conditions, Se(-II) as HSe- is the thermodynamically stable form, with behavior similar to that of sulfide (Johnson, 2004).

Selenium has six stable isotopes: $^{74}Se$, $^{76}Se$, $^{77}Se$, $^{78}Se$, $^{80}Se$ and $^{82}Se$ with relative molar proportions varying from 0.8% ($^{74}Se$) to 49.6% ($^{80}Se$) (Coplen et al., 2002). Experimental work has shown that Se isotope fractionation occurs during reduction of Se(VI) or Se(IV) to Se(0) and/or Se(-II), through various biotic or abiotic reactions (Krouse and Thode, 1962; Rees and Thode, 1966; Rashid and Krouse, 1985; Johnson et al., 1999; Herbel et al., 2000; Ellis et al., 2003). Fractionation may vary from 7‰ to 11‰ in the $\delta^{82}Se$ value, depending on environmental conditions (e.g. reducing agents, Se concentration), with the reduced product being depleted in heavier isotopes. Reduction experiments in the presence of natural sediment slurries have also yielded similar fractionation factors for Se(VI) reduction (2.6–3.1‰) and for Se(IV) reduction (5.5–5.7‰) to those performed on pure cultures (Herbel et al., 2002). Thus, substantial isotopic fractionation suggests that Se isotopes may be a powerful paleo-environmental proxy, as has been established for Mo and Fe isotopes (Anbar and Rouxel, 2007).

Based on above Se isotopic framework, greater isotope fractionation should presumably occur under anoxic and euxinic conditions when dissolved Se in the water column is reduced by microbial or abiotic processes. However, an important implication for Se is the lack of strong enrichment in light isotopes evident in most marine sediments deposited under anoxic and even euxinic conditions (Hagiwara, 2000; Mitchell et al., 2012). For example, Mitchell et al. (2012) analysed ~120 samples

* Corresponding author. Tel.: +86 851 5891723.
*E-mail address:* wenhanjie@vip.gyig.ac.cn (H. Wen).

http://dx.doi.org/10.1016/j.chemgeo.2014.10.022
0009-2541/

of fine-grained marine sedimentary rocks and sediments spanning the entire Phanerozoic, and they found that $\delta^{82}$Se values fall within a narrow range, from −1 to +1‰. This phenomenon was also observed by Hagiwara (2000) in a survey of marine sediments and algae. For unweathered (fresh) black shale samples, the mean $\delta^{82}$Se value is −0.30 ± 1.01‰ with a mean Se concentration of 77 ± 3.49 ppm; however, weathered samples yield a $\delta^{82}$Se value of 3.98 ± 3.90‰ and mean Se concentration of 716 ± 1670 ppm. The largest range of Se isotopic composition for a single sedimentary formation is reported in the Yutangba Se deposit, where supergene alteration has produced a fractionation of ~23‰ (Wen and Carignan, 2011; Zhu et al., 2014). It appears that in most cases only secondary alteration (weathering, diagenesis) can lead to a greater isotopic fractionation and Se enrichment. Overall, results from analyzed shales and sediments have not yet shown that marine sedimentary Se isotope ratios provide an indication of past redox conditions. For this reason, we report on systematic measurements of Se isotopes in some Cambrian strata. Results from Fe speciation measurements indicate that isotopically lighter Se is associated with ferruginous waters, and therefore we propose that strongly negative $\delta^{82}$Se values may be indicative of ferruginous conditions in the sedimentary record.

## 2. Geological setting and stratigraphy

The Ediacaran to early Cambrian successions were well preserved over the Yangtze platform in South China with different stratigraphical settings, including platform facies, transition belt and protected basin as illustrated in Fig. 1-a (Steiner et al., 2001; Guo et al., 2007). In several areas, they are exposed across a transection from platform to basin, offering an opportunity to investigate the stratigraphic features during this critical interval in Earth history, which can provide clues of sea-level fluctuations, ocean anoxia, metal accumulation and corresponding ocean-atmosphere-biology evolution. Three sections were selected for this study, the Huangjiawan (HJW), Chuanyanping (CYP) and Silikou (SLK) sections, which are separated from each other by approximately 400 km (Fig. 1-a), and located at sites from the carbonate platform (HJW section and CYP section) and protected basin (SLK section)

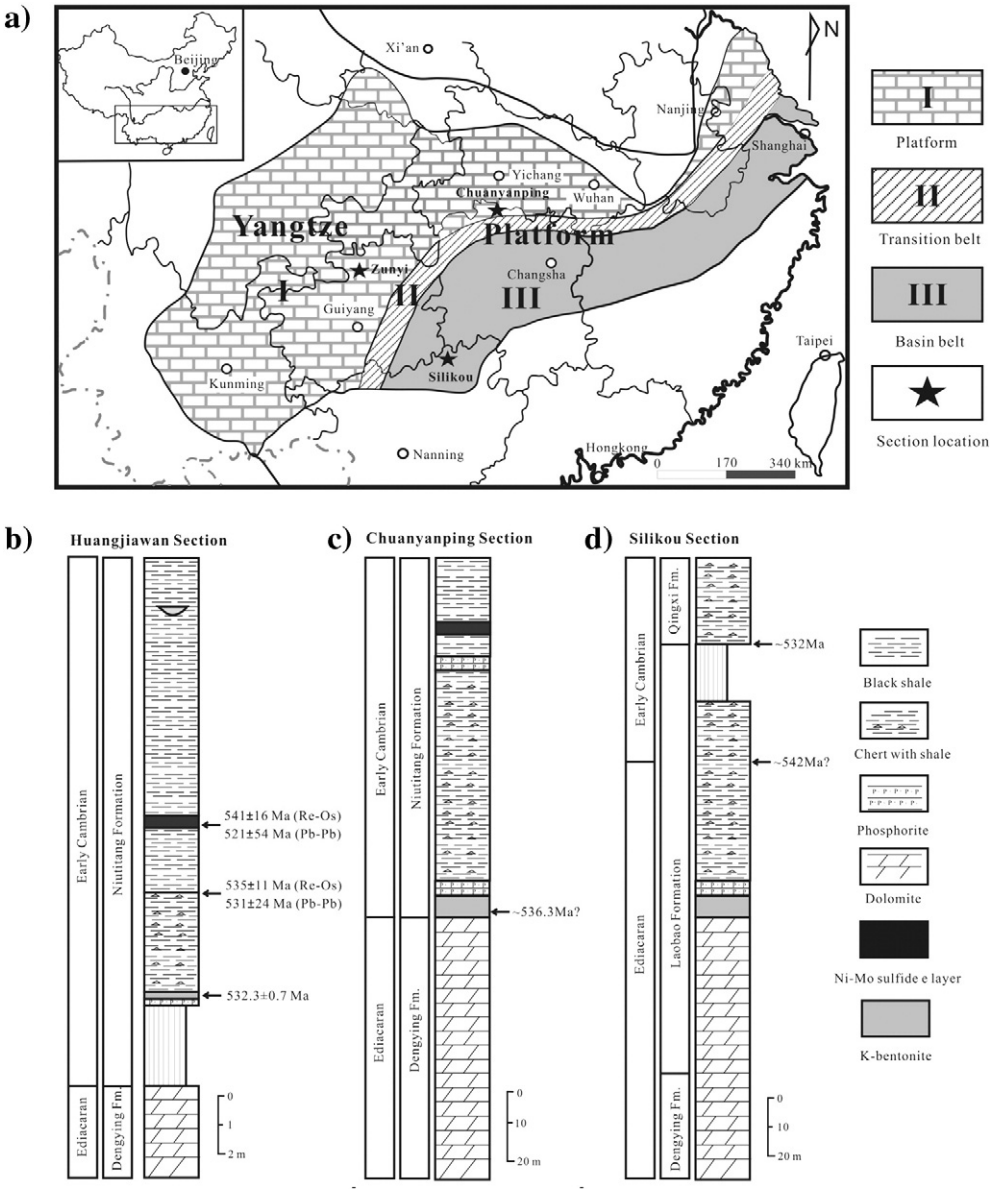


**Fig. 1.** (a) Simplified palaeogeographic map of the Yangtze Platform during Ediacaran–Cambrian transition modified from Steiner et al. (2001); (b) Lithological profile of the Huangjiawan section; (c) Lithological profile of the Chuanyanping section from Fan et al. (2013); (d) Lithological profile of the Silikou section from Chang et al. (2012).

respectively, which reflects a shallow to deep water sedimentation as documented by Zhu et al. (2007).

### 2.1. The Huangjiawan section

The Huangjiawan section is located at Huangjiawan village in Zunyi County, northern Guizhou province. The base of this section comprises dolomites of the Ediacaran (Neoproterozoic) Dengying Formation, which are disconformably overlain by the Cambrian Niutitang Formation (Fig. 1-b). A variable rock assembly occurs in the Niutitang formation, consisting of phosphorite, K-bentonite, carbonaceous shale and carbonaceous chert. Phosphorite with a thickness of several centimeters overlaid disconformably over the dolomite of the Dengying Formation. Higher up the section, the special K-bentonite layer is identified with normally several centimetres thick. Over the K-bentonite, black shale is divided into lower and upper sections by a Ni-Mo sulfide layer. The lower section comprises laminated black shales and carbonaceous chert with phosphoric nodules, in alternating layers. The upper section commonly consists of carbonaceous shales with an occasional interlayer of stone coal.

There is a discrepancy between the ages obtained for the section. Re-Os and Pb-Pb dating yielded ages of 535 ± 11 Ma (Re-Os) and 531 ± 24 Ma (Pb-Pb) for the black shales within the Niutitang Formation, and 521 ± 54 Ma (Pb-Pb) for the Ni-Mo sulfide layer (Jiang et al., 2006, 2007). This is in contrast to the Re-Os isochron age (541 ± 16 Ma) measured by Mao et al. (Mao et al., 2002). Furthermore, a much younger U-Pb zircon age (518 ± 5 Ma) was obtained for K-bentonite, which is stratigraphically lower than the black shales and Ni-Mo sulfide layer of the Niutitang Formation (Zhou et al., 2008). Further, a new U-Pb zircon age (532.3 ± 0.7 Ma) was also obtained for K-bentonite (Jiang et al., 2009). In consideration of the stratigraphic relationship, we suggest that the ages from (Jiang et al., 2006, 2007, 2009) are more reasonable than those measured by Mao et al. (2002) and Zhou et al. (2008).

### 2.2. The Chuanyanping section

The Chuanyanping section has a similar stratigraphical horizon and rock assemblages with the Huangjiawan Section, separated from each other by a distance of approximately 400 km (Fig. 1-c). The Chuanyanping section crosses the Ediacaran - early Cambrian (E-C) boundary. It includes the upper part of the Ediacaran Doushantuo and the Dengying Formation and the lower part of Cambrian Niutitang Formation, representing a shallow shelf depositional environment (Fan et al., 2013). The major lithofacies of the Dengying Formation is gray carbonates. The lower Cambrian Niutitang Formation consists of black-gray cherts, organic-rich shale succession (up to 100 m thick) and a basal Ni–Mo sulfide-rich horizon (Steiner et al., 2001). In the region, one SHRIMP U–Pb zircon age has been obtained, 536.3 ± 5.5 Ma for the tuff layer (Chen et al., 2009), which is equivalent to the E-C boundary age (542 Ma).

### 2.3. The Silikou section

The Silikou section studied here is located at Silikou village in Sanjiang Dong Autonomous County, northern Guangxi (Fig. 1-d). It comprises the upper part of the Ediacaran Doushantuo Formation, the Laobao Formation and the lower part of the Cambrian Qingxi Formation up section (Chang et al., 2012). Because of lack of rocks suitable for isotopic dating, the age of the Laobao Formation can be obtained only through stratigraphic correlation. It is ca. 550 Ma for the lower boundary, which corresponds to the Dengying-Doushantuo boundary (Condon et al., 2005), and ca. 536 Ma for the upper boundary in the early Cambrian (Zhu et al., 2007; Chen et al., 2009). The underlying Doushantuo Formation and overlying Qingxi Formation are conformable with the Laobao Formation. The Laobao Formation is ~169 m thick and consists of black (or gray) cherts with few interbedded carbonaceous or siliceous mudstones in the upper part. In the Silikou section, the Laobao cherts are finely laminated, have a nodular structure and undulating bedding surface, and contain many paleobotanical microfossils.

## 3. Samples and methods

Samples were collected from three Chinese stratigraphic sections, described above. Samples from the Huangjiawan and Chuanyanping sections were collected in underground mines. Zhu et al. (2014) found that Se isotopes vary widely as deep as 80 m below the land surface due to alteration by groundwater infiltration, but little at greater depth in the Yutangba Se deposit. In this study, mines for sample collection are located in 300-400 meters below the mountain surface, and the active ground water flow is commonly as deep as several ten meters of the land surface. In addition, the Ni-Mo sulfide layer co-existed in the black shale also kept the original structure without altered minerals found (eg. Fe oxides), ensuring that most fresh samples were obtained in these two sections. The characteristics of these samples have been described in Wen and Carignan (2011) and Fan et al. (2011, 2013). Samples from the Silikou section have been studied in detail in terms of mineralogy and petrology (Chang et al., 2010, 2012). The samples (mainly chert) have finely laminated fabric, aphanitic or microcrystalline structure. Metasomatic relict texture or distinct recrystallization is not found (Chang et al., 2010). In addition, the H/C atomic ratio of kerogen in samples exceeds 0.2 (Hu, 2008), indicating that maturity of the kerogen is low and samples experienced little thermal alteration. These results suggest that the samples from the Silikou section did not suffer a strong thermal metamorphism, distinct metasomatism or recrystallization, and thus primary deposition information may be preserved and recorded in the samples. A total of 59 samples were analysed for major and trace elements and Se isotopes. Prior to geochemical analyses, each sample was cleaned with distilled water and dried, then crushed to –200 meshes. Chemical analyses were performed using different methods.

Major and trace elements in samples were analysed by XRF (Axios, PW4400) and ICP-MS (PE Elan 9000), respectively, at the State Key Lab of Ore Deposit Geochemistry (SKLODG), Institute of Geochemistry of Chinese Academy of Sciences. Analytical uncertainty for elemental concentrations was generally better than 5%. Total organic C and total S contents in the samples were measured by C-S element analytical instrument (CS-314) in the analytical centre of the Institute of Geochemistry, Chinese Academy of Sciences. Se contents were determined by Atomic Absorption Spectrometry (Varian AAS 240 at CRPG, France) following the method of Marin et al. (2001). Pyrite iron ($Fe_P$) concentrations were analysed using the chromium reduction method, and reactive iron (HCl-extractable iron, $Fe_H$) is extracted by a boiling 12 N HCl solution method as described by Poulton and Canfield (2005) and Canfield et al. (2007).

The analytical process for Se isotopes has been detailed described by Wen and Carignan (2011). Briefly, Chemical purification of Se for isotopic measurements used the Thiol Cotton Fibre (TCF) method (Marin et al., 2001; Rouxel et al., 2002) for which Se recovery is >98%. Se isotopic measurements were performed at the Centre de Recherches Pétrographiques et Géochimiques (CRPG, France) using an Isoprobe MC-ICP-MS coupled with on-line hydride generation. Before entering the ICP torch, the Se hydrides were passed through a pneumatic nebulizer and a cyclonic chamber to further regulate the gas sample flux into the mass spectrometer. The sample-standard bracketing method was used to calculate delta values. A solution blank signal was subtracted for all measured masses (76, 77, 78, 80, and 82). Instrumental drift was corrected by averaging the measured ratios of the bracketing reference Se samples (bracketing standards). Only sections presenting linear or smooth drifts of the measured reference solution were considered and used for calculating sample delta values. The sensitivity achieved using the on-line hydride generation is ~85 V $ppm^{-1}$

total Se. A single bracket analysis comprised three blocks of 25 cycles of measurements on each amu, which corresponds to ~450 ng Se analysed. Analytical precision was better than 0.2 per ml (2σ) as described by Wen and Carignan (2011). Because there are no certificated international Se isotopic standard reference materials, the NIST SRM 3149 was used here as the "delta zero" reference material as suggested by Carignan and Wen (2007). The delta values are expressed as:

$$\delta^{82}\mathrm{Se}(‰) = \left[\left(^{82}\mathrm{Se}/^{76}\mathrm{Se}\right)_{\mathrm{sample}}/\left(^{82}\mathrm{Se}/^{76}\mathrm{Se}\right)_{\mathrm{std}} - 1\right] \times 1000$$

where std is the NIST SRM 3149 reference.

## 4. Results

The $\delta^{82/76}$Se values and selenium concentrations from the three analyzed sections, with total sulfur, organic carbon, Fe speciation and elemental enrichment ratios, are presented in Tables 1, 2 and 3. The Se isotopic compositions for all samples, with some natural sample values from the literature for comparison, are illustrated in Fig. 2.

Samples from three sections showed the distinct Se concentrations and Se isotopic compositions. The $\delta^{82}$Se and Se concentrations measured for samples from the Huangjiawan section are shown in Table 1 and Fig. 3. A high level of Se was observed in the Huangjiawan section with the range from 1.41 ppm to 221 ppm. The total range in $\delta^{82}$Se values (0.6‰ to −5.09‰ with a mean of −1.5‰, Table 1). There is no clear relationship found with Se contents. The $\delta^{82}$Se and Se concentrations in Chuanyanping samples are listed in Table 2 and Fig. 3. The Se level observed in whole rock samples is lower than that observed in Huangjiawan samples, and is normally <20 ppm (1.37–20.78 ppm). The total range in $\delta^{82}$Se values (0.86‰ to -2.02‰ with a mean of -0.94‰), which have a significantly narrower range compared with the other two sections. Although mean Se content is lowest in the Silikou section (Table 3 and Fig. 3), varying from 0.50 ppm to 6.28 ppm, a moderate variation in $\delta^{82}$Se values was measured (0.49‰ to −3.25‰) with a mean of -1.03‰.

Fe speciations have been widely used to distinguish the redox condition of water column (Poulton and Canfield, 2005; Canfield et al., 2007). Studies have shown that, if conditions were anoxic ($Fe_{HR}/Fe_T > 0.38$), low associated $Fe_{py}/Fe_{HR}$ ratios (<0.8) would indicate ferruginous bottom waters; whereas, high $Fe_{py}/Fe_{HR}$ points to euxinic conditions, or an anoxic and $H_2S$-containing water column (Li et al., 2010). Fig. 4 illustrates depositional conditions using the fractional abundance of Fe speciation in the studied strata. Data from the three sections clearly show non-uniform redox conditions. Besides some of the associated Fe that plots in the oxic and euxinic fields, most of samples, especially from the Silikou and Huangjiawan sections, plot in the ferruginous zone, as noted for Fe(II)-rich samples from Huangjiawan.

## 5. Discussions

### 5.1. Selenium isotopic system from the E–C boundary

Se/S mass ratios and $\delta^{82}$Se in the studied strata show a broadly negative correlation (Fig. 5) which suggests that Se isotope fractionation is closely related to Se and S geochemical cycles in the oceans. Seawater contains very low Se concentrations (about 0.08 ppb in modern seawater) and Se/S ratios (about $10^{-8}$ to $10^{-9}$) (Measures and Burton, 1980) while Se/S ratios in sediments are higher (>$10^{-5}$) (Hattori et al., 2004). A number of investigations have shown that Se and S cycles in the oceans exhibit marked differences, although the two elements share chemical similarities (Johnson, 2004). Se may be influenced greatly by fluxes of organically-bound Se; whereas, the marine S cycle is dominated by sulfate. It has been suggested by Cutter (1982) and Baines et al. (2001) that uptake or absorption of Se by algae/plankton and its subsequent deposition is one of the most effective mechanisms of concentrating Se in sediments to several orders of magnitude greater than seawater. This notion is also supported by measurements of modern marine plankton (typically 0.5–3 ppm Se), which indicate an enrichment of more than three orders of magnitude of Se in plankton compared with bulk seawater (Boisson and Romeo, 1996). Therefore, Se may be enriched in organic-rich black shales formed in anoxic basins with a relatively higher Se/S ratio ($10^{-5}$ to $10^{-3}$) in comparison with most clastic sedimentary rocks and evaporates ($10^{-6}$ to $10^{-5}$) (Hattori et al., 2004). As investigated through experiments and analyses of natural terrestrial samples, uptake or adsorption of Se by algae/plankton (assimilation) induces little isotopic fractionation within the range of 1‰ to 2‰ (Johnson, 2004; Clark and Johnson, 2010; Mitchell et al., 2012).

In this study, however, significant isotopic fractionation and anomalously high Se/S ratios ($10^{-3}$ to $10^{-1}$) were found in anoxic and ferruginous strata from the Silikou and Huangjiawan sections but not in euxinic sediments (e.g. Chuanyanping section and most of the reference data) (Fig. 5). Fig. 6-a clearly shows that the Se/S ratio in samples from anoxic and ferruginous conditions is closely related to the $Fe_{Py}/Fe_{HR}$ ratio. Where the $Fe_{Py}/Fe_{HR}$ ratios increase towards euxinic conditions, the Se/S ratio is in a restricted range: $10^{-4}$ to $10^{-3}$. However, where $Fe_{Py}/Fe_{HR}$ ratios are small (especially less than 0.2), elevated Se/S ratios (>$10^{-3}$) and greater variations ($10^{-3}$ to $10^{-1}$) were observed. It is consistent with the relationship between $Fe_{Py}/Fe_{HR}$ and Se isotopes (Fig. 6-b). $\delta^{82}$Se values stabilise to between −2‰ and 1‰ when $Fe_{Py}/Fe_{HR}$ increases towards euxinic conditions. However, where $Fe_{Py}/Fe_{HR}$ is <0.2, a large fractionation in Se isotopes was found (~0‰ to −5‰), as well as enrichment of the lighter isotopes, which indicate that anoxic and ferruginous conditions strongly control both the variation in Se/S ratios and the large Se isotopic fractionation. Two important implications can be observed in Fig. 6-a and 6-b: (1) the euxinic samples from the three sections show lower Se/S ratio and a narrow range

**Table 1**
Selenium isotopic compositions and Fe speciations in samples from the Huangjiawan section.

| Sample No. | Sample type | $\delta^{82/76}$Se (2σ, ‰) | S (%) | Se (ppm) | TOC (/%) | $Fe_T$ (%) | $Fe_{Py}$ (%) | $Fe_{HCl}$ (%) | $Fe_{HR}$ (%) | $Fe_{Py}/Fe_{HR}$ | $Fe_{HR}/Fe_T$ | $Fe_{HCl}/Fe_T$ | Se/S($10^{-3}$) |
|---|---|---|---|---|---|---|---|---|---|---|---|---|---|
| xiaozhu-02 | Carbonaceous shale | 0.68 ± 0.09 | 1.10 | 6.29 | 4.3 | 3.11 | 0.611 | 1.038 | 1.649 | 0.371 | 0.530 | 0.333 | 0.57 |
| xiaozhu-19 | Carbonaceous shale | −3.10 ± 0.18 | 0.25 | 116.00 | 15.9 | 2.57 | 0.062 | 1.639 | 1.701 | 0.036 | 0.662 | 0.638 | 46.08 |
| xiaozhu-20 | Carbonaceous chert | −1.40 ± 0.12 | 0.15 | 36.00 | 8.9 | 0.68 | 0.011 | 0.234 | 0.245 | 0.045 | 0.363 | 0.347 | 23.34 |
| xiaozhu-22 | Carbonaceous chert | −0.18 ± 0.06 | 0.14 | 35.00 | 7.7 | 1.31 | 0.028 | 0.749 | 0.777 | 0.036 | 0.592 | 0.570 | 24.52 |
| xiaozhu-23 | Carbonaceous shale | −5.09 ± 0.24 | 0.32 | 121.00 | 15.5 | 1.67 | 0.032 | 1.187 | 1.220 | 0.026 | 0.730 | 0.711 | 38.28 |
| xiaozhu-24 | Carbonaceous chert | −0.15 ± 0.08 | 0.16 | 26.00 | 9.1 | 0.62 | 0.033 | 0.269 | 0.302 | 0.109 | 0.485 | 0.432 | 16.12 |
| xiaozhu-25 | Carbonaceous shale | −0.27 ± 0.06 | 0.50 | 98.00 | 18.6 | 2.53 | 0.112 | 1.104 | 1.216 | 0.092 | 0.480 | 0.436 | 19.57 |
| xiaozhu-26 | Carbonaceous chert | −0.87 ± 0.10 | 0.15 | 20.00 | 8.5 | 0.71 | 0.006 | 0.341 | 0.346 | 0.016 | 0.490 | 0.482 | 13.04 |
| xiaozhu-27 | Carbonaceous shale | −3.65 ± 0.23 | 0.28 | 53.00 | 20.2 | 1.79 | 0.030 | 1.163 | 1.193 | 0.025 | 0.666 | 0.650 | 19.03 |
| xiaozhu-28 | Carbonaceous chert | −0.20 ± 0.09 | 0.09 | 8.87 | 3.4 | 0.70 | 0.004 | 0.194 | 0.197 | 0.018 | 0.282 | 0.277 | 10.07 |
| GZW-02-32 | Phosphorite | −2.21 ± 0.14 | 0.09 | 1.41 | 0.34 | 1.93 | 0.008 | 1.278 | 1.285 | 0.006 | 0.666 | 0.662 | 1.64 |

Note: $Fe_T$, $Fe_{Py}$ and $Fe_{HCl}$ represent total iron concentrations, pyrite iron concentration and HCl-extractable iron concentration in samples, respectively. $Fe_{HR}$ represents the sum of $Fe_{Py}$ and $Fe_H$.

**Table 2**
Selenium isotopic compositions and Fe speciations in samples from the Chuanyanping section.

| Sample No. | Sample type | $\delta^{82/76}$Se (2σ, ‰) | S (%) | Se (ppm) | TOC (/%) | $Fe_T$ (%) | $Fe_{Py}$ (%) | $Fe_{HCl}$ (%) | $Fe_{HR}$ (%) | $Fe_{Py}/Fe_{HR}$ | $Fe_{HR}/Fe_T$ | $Fe_{HCl}/Fe_T$ | $Se/S(10^{-3})$ |
|---|---|---|---|---|---|---|---|---|---|---|---|---|---|
| ZJJ-03 | Carbonaceous shale | −1.59 ± 0.12 | 4.53 | 8.12 | 7.47 | 2.91 | 1.745 | 0.260 | 2.004 | 0.871 | 0.690 | 0.089 | 0.18 |
| ZJJ-04 | Carbonaceous shale | −0.87 ± 0.13 | 3.38 | 11.42 | 7.14 | 2.84 | 1.140 | 0.240 | 1.380 | 0.826 | 0.487 | 0.085 | 0.34 |
| ZJJ-05 | Carbonaceous shale | −1.32 ± 0.16 | 4.85 | 13.55 | 8.13 | 2.97 | 1.014 | 0.247 | 1.261 | 0.804 | 0.425 | 0.083 | 0.28 |
| ZJJ-12 | Carbonaceous shale | −0.43 ± 0.10 | 3.28 | 5.80 | 8.36 | 2.02 | - | - | - | - | - | - | 0.18 |
| ZJJ-13 | Carbonaceous shale | −0.20 ± 0.09 | 3.25 | 5.16 | 9.08 | 2.53 | 0.591 | 0.988 | 1.579 | 0.374 | 0.625 | 0.391 | 0.16 |
| ZJJ-14 | Carbonaceous shale | −0.60 ± 0.10 | 1.67 | 4.31 | 9.82 | 1.86 | 0.578 | 1.141 | 1.718 | 0.336 | 0.924 | 0.613 | 0.26 |
| ZJJ-15 | Carbonaceous shale | −2.02 ± 0.17 | 1.86 | 9.20 | 10.32 | 1.18 | - | - | - | - | - | - | 0.49 |
| ZJJ-16 | Carbonaceous shale | −1.39 ± 0.14 | 1.24 | 5.00 |  | 1.19 | - | - | - | - | - | - | 0.4 |
| ZJJ-52 | Carbonaceous shale | −1.41 ± 0.20 | 4.40 | 7.07 | 7.12 | 3.675 | 0.703 | 1.278 | 1.981 | 0.355 | 0.539 | 0.348 | 0.16 |
| ZJJ-17 | Carbonaceous shale | −0.90 ± 0.11 | 3.21 | 8.10 | 9.23 | 1.86 | - | - | - | - | - | - | 0.25 |
| ZJJ-18 | Carbonaceous shale | −1.67 ± 0.14 | 4.03 | 6.55 | 7.65 | 4.81 | 0.923 | 0.382 | 1.305 | 0.707 | 0.271 | 0.080 | 0.16 |
| ZJJ-19 | Carbonaceous shale | −1.75 ± 0.16 | 5.27 | 18.11 | 8.3 | 3.30 | 0.702 | 0.092 | 0.795 | 0.884 | 0.240 | 0.028 | 0.34 |
| ZJJ-20 | Carbonaceous shale | −1.69 ± 0.13 | 3.84 | 12.80 | 6.34 | 2.59 | - | - | - | - | - | - | 0.33 |
| ZJJ-22 | Carbonaceous shale | −1.80 ± 0.20 | 2.48 | 6.61 | 6.36 | 2.58 | 1.486 | 0.315 | 1.801 | 0.825 | 0.697 | 0.122 | 0.27 |
| ZJJ-23 | Carbonaceous shale | −1.50 ± 0.10 | 4.39 | 14.07 | 6.86 | 2.65 | 2.37 | 0.21 | 2.58 | - | - | - | 0.32 |
| ZJJ-24 | Carbonaceous shale | −1.26 ± 0.06 | 3.39 | 18.41 | 8.52 | 2.77 | 1.937 | 0.717 | 2.653 | 0.730 | 0.957 | 0.259 | 0.54 |
| ZJJ-26 | Phosphorite | −0.16 ± 0.06 | 0.65 | 20.78 | 0.91 | 2.20 | 0.285 | 0.034 | 0.318 | 0.894 | 0.145 | 0.015 | 3.21 |
| ZJJ-27 | Carbonaceous chert | 0.56 ± 0.10 | 0.33 | 4.35 | 0.13 | 0.40 | - | - | - | - | - | - | 1.31 |
| ZJJ-28 | Carbonaceous chert | 0.86 ± 0.11 | 0.19 | 3.63 | 0.76 | 1.30 | 0.055 | 0.082 | 0.137 | 0.402 | 0.105 | 0.063 | 1.87 |
| ZJJ-43 | Carbonaceous chert | −0.62 ± 0.10 | 0.26 | 1.37 | 0.09 | 0.46 | 0.016 | 0.101 | 0.117 | 0.136 | 0.253 | 0.219 | 0.52 |
| ZJJ-56 | Carbonaceous chert | 0.00 ± 0.05 | 0.66 | 8.36 | 0.54 | 0.77 | 0.014 | 0.359 | 0.374 | 0.038 | 0.485 | 0.467 | 1.27 |

Note: $Fe_T$, $Fe_{Py}$ and $Fe_{HCl}$ represent total iron concentrations, pyrite iron concentration and HCl-extractable iron concentration in samples, respectively. $Fe_{HR}$ represents the sum of $Fe_{Py}$ and $Fe_H$.

(−2‰ to 0‰) in $\delta^{82}$Se value; (2) although the Se/S ratio in samples from oxic conditions is variable, isotopic fractionation is also limited to between −2‰ and 1‰ in $\delta^{82}$Se value. The HCl-Fe commonly includes Fe-(oxyhydr) oxides, ferrous carbonates (e.g. siderite and ankerite) and some Fe from certain sheet silicate minerals (e.g. nontronite, chlorite, glauconite, biotite). In anoxic condition, the high $Fe_H/Fe_T$ ratio represents the excessive Fe(II) occurred in the water column. A broadly negative correlation between $\delta^{82}$Se values and $Fe_H/Fe_T$ can be observed for anoxic and ferruginous samples in Fig. 6-c, however, most of euxinic and oxic samples do not array in this trend. Therefore, it is evident that lower $Fe_{Py}/Fe_{HR}$ ratios in anoxic conditions represent the presence of excess Fe(II) in the water column, which may be responsible for the larger Se isotopic fractionation, thereby facilitating the enrichment of lighter isotopes.

### 5.2. Mechanism of Se isotopic variations in ferruginous waters

Although microbial action is reported to be an important, and likely dominant, oxyanion reduction and removal pathway of Se, recent research has identified that abiotic redox reactions also play an important

**Table 3**
Selenium isotopic compositions and Fe speciations in samples from the Silikou section.

| Sample No. | Sample type | $\delta^{82/76}$Se (2σ, ‰) | S (%) | Se (ppm) | TOC (/%) | $Fe_T$ (%) | $Fe_{Py}$ (%) | $Fe_{HCl}$ (%) | $Fe_{HR}$ (%) | $Fe_{Py}/Fe_{HR}$ | $Fe_{HR}/Fe_T$ | $Fe_{HCl}/Fe_T$ | $Se/S(10^{-3})$ |
|---|---|---|---|---|---|---|---|---|---|---|---|---|---|
| **Sampling site: Silikou section** | | | | | | | | | | | | | |
| SLK-117 | chert | −0.36 ± 0.08 | 0.049 | 2.28 | 0.41 | 0.70 | 0.002 | 0.190 | 0.192 | 0.010 | 0.274 | 0.271 | 4.65 |
| SLK-111 | chert | −1.10 ± 0.12 | 0.034 | 1.05 | 2.30 | 0.48 | nd | - | - | - | - | - | 3.08 |
| SLK-107 | chert | −0.57 ± 0.09 | 0.545 | 1.39 | 1.98 | 0.79 | 0.206 | 0.210 | 0.416 | 0.495 | 0.527 | 0.266 | 0.26 |
| SLK-103 | chert | 0.15 ± 0.06 | 0.469 | 2.30 | 2.71 | 0.52 | 0.234 | 0.200 | 0.434 | 0.539 | 0.835 | 0.385 | 0.49 |
| SLK-94 | chert | −2.53 ± 0.14 | 0.013 | 0.95 | 1.02 | 0.31 | nd | - | - | - | - | - | 7.31 |
| SLK-90 | chert | −1.04 ± 0.11 | 0.132 | 0.99 | 1.65 | 0.48 | 0.041 | 0.200 | 0.241 | 0.170 | 0.502 | 0.417 | 0.75 |
| SLK-87 | chert | −0.46 ± 0.08 | 0.051 | 2.08 | 2.22 | 0.48 | 0.001 | 0.120 | 0.121 | 0.008 | 0.252 | 0.250 | 4.07 |
| SLK-85 | chert | −0.29 ± 0.06 | 0.043 | 0.28 | 2.96 | 0.41 | nd | - | - | - | - | - | 0.66 |
| SLK-83 | chert | −0.73 ± 0.09 | 0.113 | 1.63 | 5.12 | 0.32 | 0.001 | 0.120 | 0.121 | 0.008 | 0.378 | 0.375 | 1.44 |
| SLK-78 | chert | 0.49 ± 0.10 | 0.364 | 1.89 | 0.86 | 0.83 | 0.101 | 0.210 | 0.311 | 0.325 | 0.375 | 0.253 | 0.52 |
| SLK-71 | chert | −1.47 ± 0.12 | 0.035 | 1.71 | 1.82 | 0.36 | nd | - | - | - | - | - | 4.89 |
| SLK-59 | chert | −1.93 ± 0.16 | 0.042 | 0.52 | 2.40 | 0.28 | nd | - | - | - | - | - | 1.25 |
| SLK-57 | chert | 1.43 ± 0.14 | 0.499 | 2.10 | 0.78 | 0.75 | 0.104 | 0.220 | 0.324 | 0.321 | 0.432 | 0.293 | 0.42 |
| SLK-53.5 | chert | −1.62 ± 0.16 | 0.044 | 1.44 | 1.64 | 0.41 | nd | - | - | - | - | - | 3.26 |
| SLK-51 | chert | −0.37 ± 0.08 | 0.306 | 1.78 | 1.72 | 0.41 | 0.069 | 0.190 | 0.259 | 0.266 | 0.632 | 0.463 | 0.58 |
| SLK-47 | chert | −1.27 ± 0.11 | 0.021 | 0.50 | 1.66 | 0.17 | nd | - | - | - | - | - | 2.39 |
| SLK-43 | chert | −1.54 ± 0.15 | 0.361 | 1.54 | 0.49 | 0.58 | 0.113 | 0.210 | 0.323 | 0.350 | 0.557 | 0.362 | 0.43 |
| SLK-40 | chert | −0.06 ± 0.07 | 0.166 | 2.22 | 0.20 | 0.43 | 0.094 | 0.190 | 0.284 | 0.331 | 0.660 | 0.442 | 1.34 |
| SLK-36 | chert | −2.34 ± 0.15 | 0.004 | 2.47 | 0.25 | 0.38 | 1 | 0.14 | 0.142 | 0.014 | 0.374 | 0.368 | 61.76 |
| SLK-31 | chert | −2.40 ± 0.18 | 0.015 | 3.04 | 0.89 | 0.36 | 0.001 | 0.16 | 0.161 | 0.006 | 0.447 | 0.444 | 20.24 |
| SLK-24 | chert | −1.16 ± 0.09 | 0.009 | 0.94 | 0.76 | 0.27 | 0.003 | 0.11 | 0.113 | 0.027 | 0.419 | 0.407 | 10.39 |
| SLK-20 | chert | −1.37 ± 0.11 | 0.008 | 1.07 | 0.60 | 0.32 | 0.002 | 0.2 | 0.202 | 0.010 | 0.631 | 0.625 | 13.33 |
| SLK-16 | chert | −0.23 ± 0.07 | 0.063 | 3.38 | 0.56 | 0.44 | 0.024 | 0.22 | 0.244 | 0.098 | 0.555 | 0.5 | 5.37 |
| SLK-12 | chert | −1.10 ± 0.10 | 0.1 | 6.28 | 0.33 | 0.47 | 0.025 | 0.26 | 0.285 | 0.088 | 0.606 | 0.553 | 6.28 |
| SLK-8 | chert | −3.25 ± 0.22 | 0.018 | 3.35 | 0.61 | 0.32 | 0.002 | 0.14 | 0.142 | 0.014 | 0.444 | 0.438 | 18.62 |
| SLK-4 | chert | −1.71 ± 0.13 | 0.007 | 2.25 | 0.79 | 0.34 | 0.001 | 0.16 | 0.161 | 0.006 | 0.474 | 0.471 | 32.14 |

Note: $Fe_T$, $Fe_{Py}$ and $Fe_{HCl}$ represent total iron concentrations, pyrite iron concentration and HCl-extractable iron concentration in samples, respectively. $Fe_{HR}$ represents the sum of $Fe_{Py}$ and $Fe_H$.

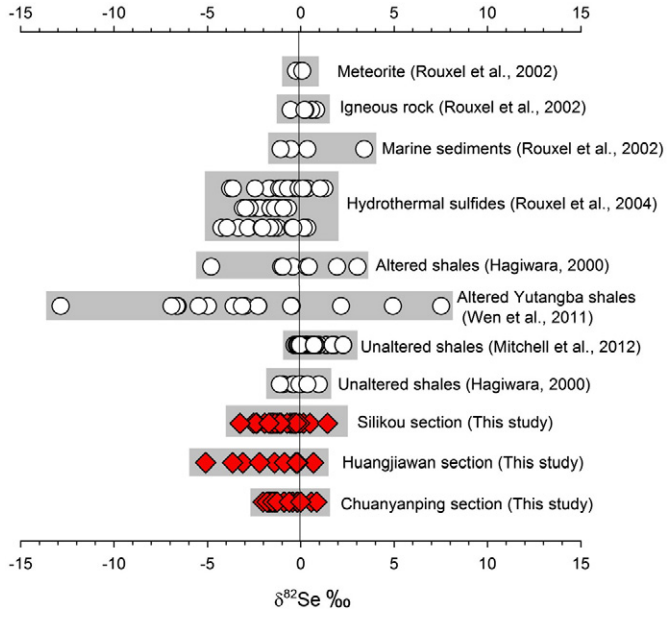


**Fig. 2.** Se isotopic variations in samples from the three analyzed sections, with natural sample values from the literature.

role in Se cycling. For example, under sulfidic conditions selenite can reductively precipitate as elemental Se as follows (Weres et al., 1989; Breynaert et al., 2008):

$$SeO_3^{2-} + 2HS^- + 4H^+ = Se^0 + 2S^0 + 3H_2O \left(\triangle G^0 = -324.3\ \text{kJ/mol}\right) \quad (1)$$

However, the elemental Se produced by the reaction may be is unstable because under the condition of an $H_2S$-containing water column, elemental Se can be readily further reduced to $H_2Se$ or $HSe^-$. An Eh-pH diagram after Brookins (1988) clearly indicates a very limited region of coexistence for hydrogen sulphides ($HS^- + H_2S$) and elemental Se, but a wide region of coexistence for hydrogen sulphides ($HS^- + H_2S$) and hydrogen selenide ($HSe^- + H_2Se$) identified by thermodynamic calculation. Field measurements by Cutter (1982) also revealed that hydrogen selenide actually occurred in the $H_2S$-containing water column. Therefore, under strongly reducing conditions, selenide would be formed by reduction in presence of hydrogen sulphides but

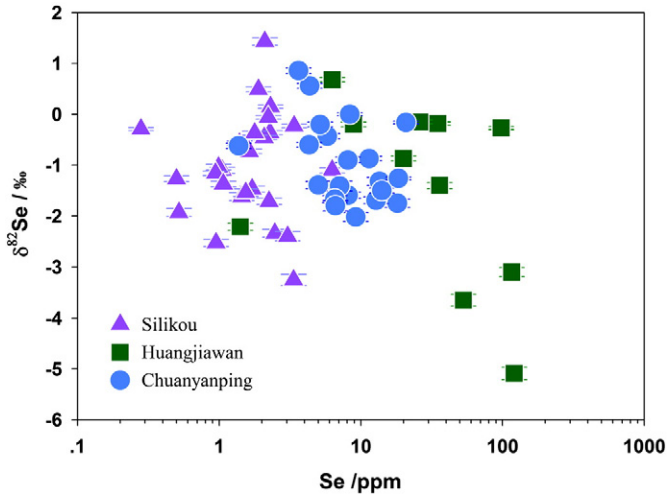


**Fig. 3.** Se isotopic variations and Se concentrations for samples from the three analysed sections.

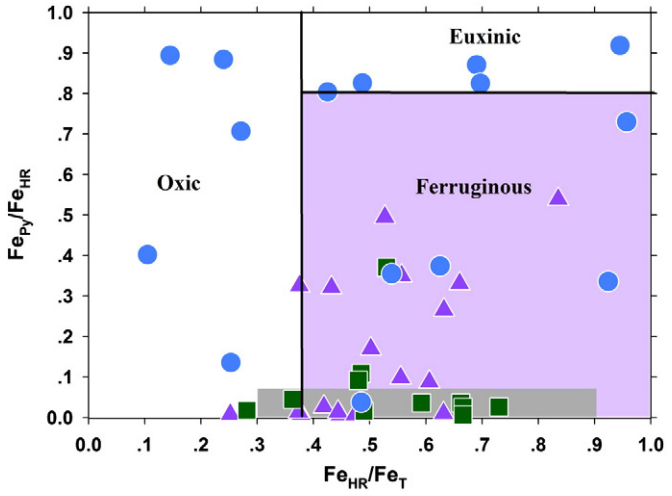


**Fig. 4.** Variations of $Fe_{Py}/Fe_{HR}$ and $Fe_{HR}/Fe_T$ data for samples from the three analysed sections, with end-member redox conditions denoted on the cross-plot (Li et al., 2010).

furthermore could be retained in a sulfidic water column because metal cations (e.g. Fe, Cu, Pb, Cd, Hg, and Ag) are scavenged by sulfide mineral formation and are therefore not available to form solid selenides. This indicates that sulfidic conditions would not cause an excess Se deposition in sediments, and then result in a higher Se/S ratio (commonly $10^{-5}$ to $10^{-3}$ similar to most organic-rich black shales formed in anoxic basins, Hattori et al., 2004). This may be the critical reason why Se isotope fractionation is limited to a certain range, based on measurements of almost all fresh natural samples from anoxic or even euxinic conditions (such as in the Chuanyanping section; see also reference data).

A number of clues suggest that the abiotic reduction of Se(VI) and/or Se(IV) by reduced Fe species (e.g. green rust [$GRSO_4$]) occurs, which may be an important process in Se cycling in nature. Experiments of abiotic Se redox transformations in the presence of Fe(II, III) oxides (GRSO4) showed that Se reduces from an oxidation state of Se(VI) to Se(0) and Se(-II) (Myneni et al., 1997). Meanwhile, reactions of elemental Fe and $Fe(OH)_2$ with Se(VI) in the laboratory produce similar redox transformations (Zingaro et al., 1997). The adsorption of Se on other

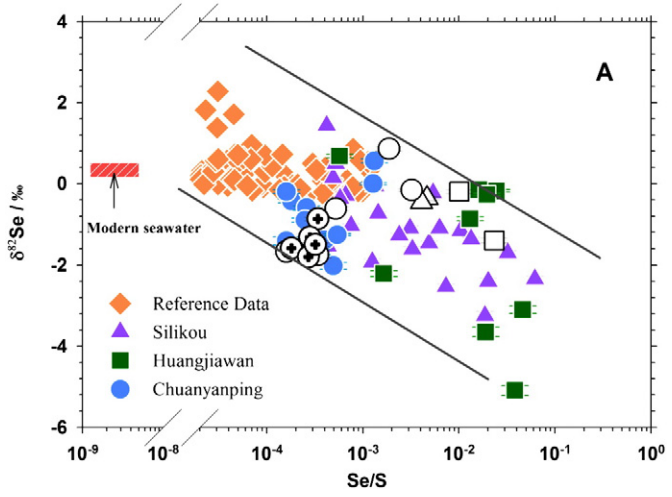


**Fig. 5.** Correlation between Se isotopic variations and Se/S ratios with reference data from Hagiwara (2000) and Mitchell et al. (2012). The seawater Se isotope value comes from estimation by Rouxel et al. (2002). Same shape represents samples from same site with different depositional conditions. Colour-filled symbols represent samples from anoxic and ferruginous conditions; open symbols represent samples from oxic conditions and crossed symbols (x) represent samples from euxinic conditions.

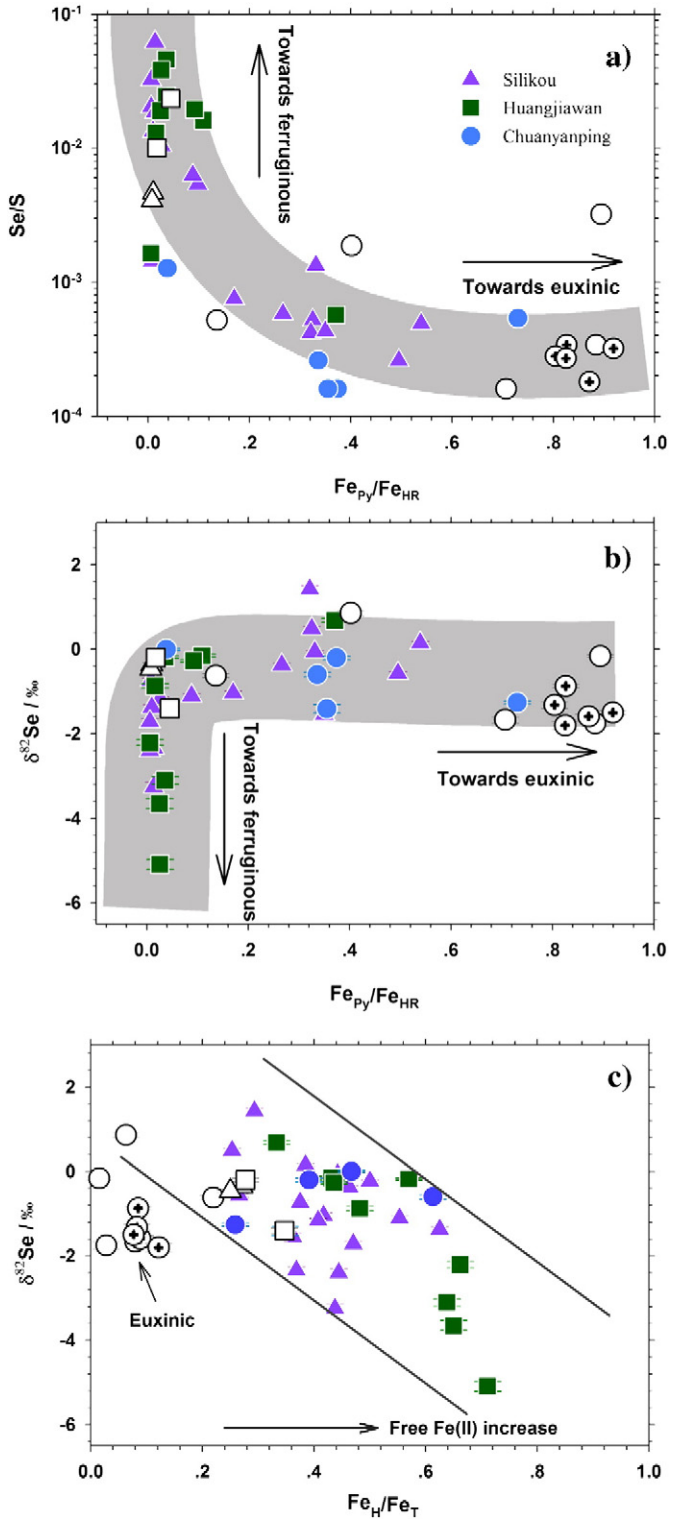


**Fig. 6.** (a) Correlation between Se/S ratio and $Fe_{Py}/Fe_{HR}$. (b) Correlation between Se isotopic variations and $Fe_{Py}/Fe_{HR}$. (c) Correlation between Se isotopic variations and $Fe_H/Fe_T$. Same shape represents samples from same site with different depositional conditions. Colour-filled symbols represent samples from anoxic and ferruginous conditions; open symbols represent samples from oxic conditions and crossed symbols (x) represent samples from euxinic conditions.

Fe-bearing mineral phases, such as Fe sulfides (pyrite) is also an effective mechanism for Se removal from solution. However, an electron transfer mechanism mediated by ferrous iron is proposed to operate during the reduction of aqueous Se(IV) by pyrite (Kang et al., 2011). Therefore, reduction by Fe(II) is likely to be an effective and important pathway for removing Se from the water column to sediments via deposition of elemental Se, or of $FeSe/FeSe_2$ as $HSe^-$ incorporating the Fe cation. These redox reactions represent an abiotic pathway for Se cycling in natural environments, which has previously been considered to be mediated principally by microorganisms. Therefore, Relative to sulfidic condition, it is reasonable to predict that the ferruginous condition in water column will effectively drive Se to reduce and precipitate, and result in an excessive accumulation of Se in sediments with an elevated Se/S ratio.

Further experiments on reduction of selenate have used $GRSO_4$ with varying solution compositions and pH, yielding identical isotopic fractionation of ~11‰ in $\delta^{82}Se$ values, which indicates that selenite reduction by $GRSO_4$, induces a much larger isotopic fractionation than that of bacterial selenite reduction (Johnson and Bullen, 2003). Similarly, Se sorption by Fe(II) sulfides could lead to relatively high fractionation (up to 9.7‰) (Mitchell et al., 2013). However, as mentioned above, burial of organically bound Se by assimilation and dissimilation is an important flux even in oceans with ferruginous waters in comparison with abiotic process (Cutter, 1982; Cutter and Bruland, 1984; Baines et al., 2001; Mitchell et al., 2012). It is necessary to note that dissimilatory microbial reduction also will yield large isotope fractionation (up to 13.7‰ in $\delta^{82}Se$ value) based on experimental measurements (Herbel et al., 2000, 2002; Ellis et al., 2003). However, the lack of strong enrichment in light isotopes in most marine sediments indicates that this process is less important than assimilation processes on Se cycling in the oceans. Therefore, this abiotic reduction of Se by Fe(II) may be major mechanism for larger Se isotopic fractionation in an ferruginous water column, and resulting in an enrichment of lighter isotopes, which is consistent with our observations from the three stratigraphic sections of this study. Although the bulk Se isotope fractionation will depend on proportions of biotic and abiotic Se fluxes in oceans with ferruginous waters, it could be concluded that the lighter Se isotopic fractionation found in sediments will indicate a stronger ferruginous oceans.

### 5.3. Implications on the seawater conditions into the Early Cambrian

Overall, our study clarifies the removal mechanism of Se from the water column under different conditions, and its possible isotopic fractionation. A schematic diagram is shown in Fig. 7 to aid in developing Se isotopes as a proxy for palaeo-environmental conditions. As observed in most studies, the diagram indicates the restricted Se isotope fractionation range (−1‰ to +1‰) that is found in most fresh natural samples. In both oxic and anoxic conditions, Se mainly occurs as organic-bound Se and also as Se adsorbed by Fe-Mn oxides, and is slightly enriched in the lighter isotope relative to the coexisting solution (Rouxel et al., 2002). Under anoxic conditions, organic-bound Se remains a major species, as observed in most organic-rich black shales (Fan et al., 2011). However, in the anoxic and $H_2S$-containing water column (sulfidic condition), the Se oxyanion can be reduced to elemental Se, and further reduced to $H_2Se$ or $HSe^-$, which is then retained in the water column due to an absence of metal cations. No greater range in Se isotope fractionation is possible in such sediments.

However, the most important result of our study is that theoretical considerations and field measurements provide the first direct evidence that only ferruginous conditions can result in excessive accumulation of Se in sediments and elevated Se/S ratios in the presence of Fe(II), thereby inducing a larger isotope fractionation. This strongly suggests that Se isotopes are an appropriate geochemical proxy to trace unique oceanic conditions within the geological record.

Abundant geochemical evidence mostly suggests that oceanic basins were fully oxygenated by the late Ediacaran (Fike et al., 2006; Scott et al., 2008). However, other studies provide seemingly conflicting evidence for a redox stratified Ediacaran ocean, and anoxic deep waters with ferruginous conditions persisting into the Cambrian (Canfield et al., 2008; Li et al., 2010). Our results of Se isotopes combined with

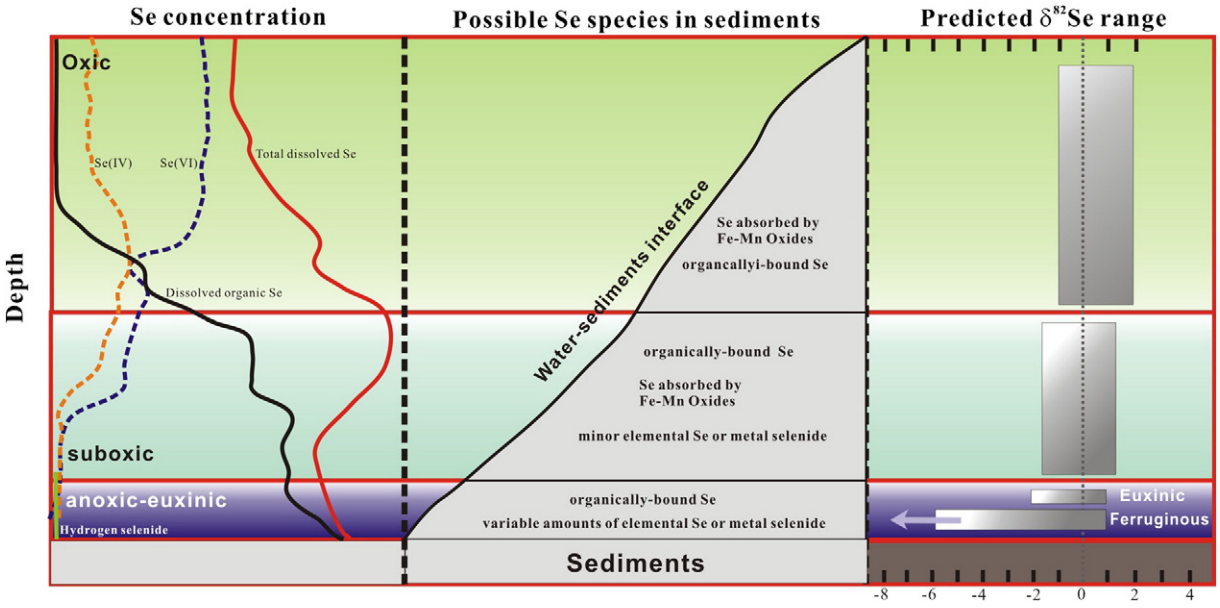


**Fig. 7.** Schematic diagrams for Se concentration and speciation in seawater along with redox conditions, possible Se speciation in sediments and predicated Se isotopic fractionation.

Fe speciation further indicates that anoxic waters with ferruginous conditions must have been present in early Cambrian ocean along the eastern margin of the Yangtze platform, although local ocean sulfidic zone may still present. This suggests that oceanic circulation was stepwise reorganized, and these changes in ocean chemistry conditions may have been responsible for triggering the biological diversification known as the Cambrian explosion. In addition, large magnitude fluctuation in Se isotope composition should also be evident during most of the Proterozoic if the proposed oceanic redox stratification model for anoxic deep waters with ferruginous conditions is feasible, but it need to develop via relevant geological strata to test our conclusion.

## 6. Conclusions

According to the presently available Se isotope framework, it is expected that redox changes in the ancient oceans would induce significant isotopic fractionation, and the Se isotopic signatures recorded in ancient sedimentary rocks might provide new insight into how the redox state of the ancient ocean has evolved. However, the hypothesis has not been verified because of the fairly narrow range (−2‰ to +2‰) in $\delta^{82}$Se value measured for most fresh sedimentary rocks. Our studies have shown that only anoxic and ferruginous conditions can result in excessive accumulation of Se in sediments with an elevated Se/S ratio and significant isotope fractionation (about 6‰), which proposed that Se isotopes are an appropriate geochemical proxy to trace unique oceanic conditions over times. Accordingly, Se isotopic variations measured in three Early Cambrian formations in southern China suggest that anoxic waters with ferruginous conditions should be mostly prevailing in early Cambrian ocean along the eastern margin of the Yangtze platform. It indicated that oceanic circulation was stepwise reorganized and may have triggered biological diversification from the Ediacaran to the Early Cambrian.

## Acknowledgments

The authors acknowledge C. Fournier (CRPG) for her help in the MC-ICP-MS laboratories and Luc Marin (CRPG) for assistance with the chemistry. This project was financially supported by 973 Program (2014CB44090X4), National Natural Science Foundation of China (Grant Nos. 40930425, 41173026), CAS/SAFEA International Partnership Program for Creative Research Teams (KZZD-EW-TZ-20), The 12th Five-Year Plan project of State Key Laboratory of Ore-deposit Geochemistry, Chinese Academy of Sciences (SKLODG-ZY125-07).

## References

Anbar, A.D., Rouxel, O., 2007. Metal stable isotopes in paleoceanography. Ann. Rev. Earth Planet. Sci. 35, 717–746.
Baines, S.B., Fisher, N.S., Doblin, M.A., 2001. Uptake of dissolved organic selenides by marine phytoplankton. Limnol. Oceanogr. 46, 1936–1944.
Boisson, F., Romeo, M., 1996. Selenium in plankton from the Northwestern Mediterranean sea. Water Res. 30, 2593–2600.
Breynaert, E., Bruggeman, C., Maes, A., 2008. XANES-EXAFS analysis of Se solid-phase reaction products formed upon contacting Se(IV) with $FeS_2$ and FeS. Environ. Sci. Technol. 42, 3595–3601.
Brookins, D.G., 1988. Eh– pH diagrams for geochemistry. Springer-Verlag, Berlin (176 pp.).
Canfield, D.E., Poulton, S.W., Narbonne, G.M., 2007. Late-Neoproterozoic deep-ocean oxygenation and the rise of animal life. Science 315, 92–95.
Canfield, D.E., Poulton, S.W., Knoll, A.H., Narbonne, G.M., Ross, G., Goldberg, T., Strauss, H., 2008. Ferruginous conditions dominated later Neoproterozoic deep-water chemistry. Science 321, 949–952.
Carignan, J., Wen, H.J., 2007. Scaling NIST SRM 3149 for Se isotope analysis and isotopic variations of natural samples. Chem. Geol. 242, 347–350.
Chang, H.J., Chu, X.L., Feng, L.J., Huang, J., 2010. Iron speciation in cherts from the Laobao Formation, South China: Implications for anoxic and ferruginous deep-water conditions. Chin. Sci. Bull. 55, 3189–3196.
Chang, H.J., Chu, X.L., Feng, L.J., Huang, J., 2012. Progressive oxidation of anoxic and ferruginous deep-water during deposition of the terminal Ediacaran Laobao Formation in South China. Palaeogeogr. Palaeoclimatol. Palaeoecol. 321–322, 80–87.
Chen, D.Z., Wang, J.G., Qing, H.R., Yan, D.T., Li, R.W., 2009. Hydrothermal venting activities in the Early Cambrian South China: petrological, geochronological and stable isotopic constraints. Chem. Geol. 258, 168–181.
Clark, S.K., Johnson, T.M., 2010. Selenium stable isotope investigation into selenium biogeochemical cycling in a lacustrine environment: Sweitzer Lake, Colorado. J. Environ. Qual. 39, 2200–2210.
Condon, D., Zhu, M., Bowring, S., 2005. U-Pb ages from the Neoproterozoic Doushantuo formation, China. Science 308, 95–98.
Coplen, T.B., Bohlke, J.K., DeBievre, P., Ding, T., Holden, N.E., Hopple, J.A., Krouse, R., Lamberty, A., Peiser, H.S., Revesz, K., Rieder, S.E., Rosman, K.J.R., Roth, E., Taylor, P.D.P., Vocke, R.D.J., Xiao, Y.K., 2002. Isotope-abundance variations of selected elements (IUPAC technical report). Pure Appl. Chem. 74, 1987–2017.
Cutter, G.A., 1982. Selenium in reducing waters. Science 217, 829–831.
Cutter, G.A., Bruland, K.W., 1984. The marine biogeochemistry of selenium: A re-evaluation. Limnol. Oceanogr. 29, 1179–1192.
Ellis, A.S., Johnson, T.M., Herbel, M.J., Bullen, T.D., 2003. Stable isotope fractionation of selenium by natural microbial consortia. Chem. Geol. 195, 119–129.
Fan, H.F., Wen, H.J., Hu, R.Z., Zhao, H., 2011. Selenium speciation in Lower Cambrian Se-enriched strata in South China and its geological implications. Geochim. Cosmochim. Acta 75, 7725–7740.
Fan, H.F., Wen, H.J., Zhu, X.K., Hua, R.Z., Tian, S.H., 2013. Hydrothermal activity during Ediacaran–Cambrian transition: Silicon isotopic evidence. Precambrian Res. 224, 23–35.
Fike, D.A., Grotzinger, J.P., Pratt, L.M., Summons, R.E., 2006. Oxidation of the Ediacaran ocean. Nature 444, 744–747.

Guo, Q.J., Shields, G.A., Liu, C.Q., Strauss, H., Zhu, M.Y., Pi, D.H., Goldberg, T., Yang, X., 2007. Trace element chemostratigraphy of two Ediacaran-Cambrian successions in South China: Implications for organosedimentary metal enrichment and silicification in the Early Cambrian. Palaeogeogr. Palaeoclimatol. Palaeoecol. 254, 194–216.
Hagiwara, Y., 2000. Selenium isotope ratios in marine sediments and algae: A reconnaissance study(Dissertation for the Master Degree) University of Illinois at Urbana-Champaign, Urbana, IL.
Hattori, K.H., Cabri, L.J., Johanson, B., Zientek, M.L., 2004. Origin of placer laurite from Borneo: Se and As contents, and S isotopic compositions. Mineral. Mag. 68, 353–368.
Herbel, M.J., Johnson, T.M., Oremland, R.S., Bullen, T.D., 2000. Fractionation of selenium isotopes during bacterial respiratory reduction of selenium oxyanions. Geochim. Cosmochim. Acta 64, 3701–3709.
Herbel, M.J., Johnson, T.M., Tanji, K.K., 2002. Selenium stable isotope ratios in California agricultural drainage water management systems. J. Environ. Qual. 31, 1146–1156.
Hu, J., 2008. The cherty microbolity in the deeper water facies during the Precambrian–Cambrian transitional period in Northeast Guangxi Province, China. Acta Micropalaeontol. Sin. 25, 291–305 (in Chinese with English abstract).
Jiang, S.Y., Chen, Y.Q., Ling, H.F., Yang, J.H., Feng, H.Z., Ni, P., 2006. Trace- and rare-earth element geochemistry and Pb-Pb dating of black shales and intercalated Ni-Mo-PGE-Au sulfide ores in Lower Cambrian strata, Yangtze Platform, South China. Miner. Deposita 41, 453–467.
Jiang, S.Y., Yang, J.H., Ling, H.F., Chen, Y.Q., Feng, H.Z., Zhao, K.D., Ni, P., 2007. Extreme enrichment of polymetallic Ni-Mo-PGE-Au in Lower Cambrian black shales of South China: An Os isotope and PGE geochemical investigation. Palaeogeogr. Palaeoclimatol. Palaeoecol. 254, 217–228.
Jiang, S.Y., Pi, D.H., Heubeck, C., Frimmel, H., Liu, Y.P., Deng, H.L., Ling, H.F., Yang, J.H., 2009. Early Cambrian ocean anoxia in South China. Nature 459, E5–E6.
Johnson, T.M., 2004. A review of mass-dependent fractionation of selenium isotopes and implications for other heavy stable isotopes. Chem. Geol. 204, 201–214.
Johnson, T.M., Bullen, T.D., 2003. Selenium isotope fractionation during reduction by Fe(II)-Fe(III) hydroxide-sulfate (green rust). Geochim. Cosmochim. Acta 67, 413–419.
Johnson, T.M., Herbel, M.J., Bullen, T.D., Zawislanski, P.T., 1999. Selenium isotope ratios as indicators of selenium sources and oxyanion reduction. Geochim. Cosmochim. Acta 63, 2775–2783.
Kang, M.L., Chen, F.L., Wu, S.J., Yang, Y.L., Bruggeman, C., Charlet, L., 2011. Effect of pH on aqueous Se(IV) reduction by pyrite. Environ. Sci. Technol. 45, 2704–2710.
Krouse, H.R., Thode, H.G., 1962. Thermodynamic properties and geochemistry of isotopic compounds of selenium. Can. J. Chem. 40, 367–375.
Li, C., Love, G.D., Lyons, T.W., Fike, D.A., Sessions, A.L., Chu, X.L., 2010. A Stratified redox model for the Ediacaran Ocean. Science 328, 80–83.
Mao, J.W., Lehmann, B., Du, A.D., Zhang, G., Ma, D., Wang, Y., Zeng, M., Kerrich, R., 2002. Re-Os dating of polymetallic Ni-Mo- PGE-Au mineralisation in Lower Cambrian black shales of South China and its geological significance. Econ. Geol. 97, 1051–1061.
Marin, L., Lhomme, J., Carignan, J., 2001. Determination of selenium concentration in sixty five reference materials for geochemical analysis by GFAAS after separation with thiol cotton. Geostand. Newslett. 25, 317–324.
Measures, C.I., Burton, J.D., 1980. The vertical distribution and oxidation states of dissolved selenium in the Northeast Atlantic ocean and their relationship to Biological Processes. Earth Planet. Sci. Lett. 46, 385–396.
Mitchell, K., Mason, P.R.D., Cappellen, P., Johnson, T.M., Gill, B.C., Owens, J.D., Diaz, J., Ingall, E.D., Reichart, G., Lyons, T.W., 2012. Selenium as paleo-oceanographic proxy: A first assessment. Geochim. Cosmochim. Acta 89, 302–317.
Mitchell, K., Couture, R.M., Johnson, T.M., Mason, P.R.D., Van Cappellen, P., 2013. Selenium sorption and isotope fractionation: Iron(III) oxides versus iron(II) sulphides. Chem. Geol. 342, 21–28.
Myneni, S.C.B., Tokunaga, T.K., Brown Jr., G.E., 1997. Abiotic selenium redox transformations in the presence of Fe(II,III) oxides. Science 278, 1106–1109.
Neal, R.H., Sposito, G., 1989. Selenate adsorption on Alluvial soils. Soil Sci. Soc. Amer. J. 53, 70–74.
Poulton, S.W., Canfield, D.E., 2005. Development of a sequential extraction procedure for iron: implications for iron partitioning in continentally derived particulates. Chem. Geol. 214, 209–221.
Rashid, K., Krouse, H.R., 1985. Selenium isotopic fractionation during $SeO_3^{2-}$ reduction to $Se^0$ and $H_2Se$. Can. J. Chem. 63, 3195–3199.
Rees, C.E., Thode, H.G., 1966. Selenium isotope effects in the reduction of sodium selenite and of sodium selenate. Can. J. Chem. 44, 419–427.
Rouxel, O., Ludden, J.N., Carignan, J., Marin, L., Fouquet, Y., 2002. Natural variations of Se isotopic composition determined by hydride generation multiple collector inductively coupled plasma mass spectrometry. Geochim. Cosmochim. Acta 66, 3191–3199.
Scott, C., Lyons, T.W., Bekker, A., Shen, Y., Poulton, S.W., Chu, X., Anbar, A.D., 2008. Tracing the stepwise oxygenation of the Proterozoic ocean. Nature 452 (7186), 456–459.
Steiner, M., Wallis, E., Erdtmann, B.D., Zhao, Y.L., Yang, R.D., 2001. Submarine-hydrothermal exhalative ore layers in black shales from South China and associated fossils - insights into a Lower Cambrian facies and bio-evolution. Palaeogeogr. Palaeoclimatol. Palaeoecol. 169, 165–191.
Wen, H.J., Carignan, J., 2011. Selenium isotopes trace the source and redox processes in the black shale-hosted Se-rich deposits in China. Geochim. Cosmochim. Acta 75, 1411–1427.
Weres, O., Jaouni, A.R., Tsao, L., 1989. The distribution, speciation and geochemical cycling of selenium in a sedimentary environment, Kesterson Reservoir, California, U.S.A. Appl. Geochem. 4, 543–563.
Zhou, M.Z., Luo, T.Y., Li, Z.X., Zhao, H., Long, H.S., Yang, Y., 2008. SHRIMP U-Pb zircon age of tuff at the bottom of the Lower Cambrian Niutitang Formation, Zunyi, South China. Chin. Sci. Bull. 53, 576–583.
Zhu, M.Y., Zhang, J.M., Yang, A.H., 2007. Integrated Ediacaran (Sinian) chronostratigraphy of South China. Palaeogeogr. Palaeoclimatol. Palaeoecol. 254, 7–61.
Zhu, J.M., Johnson, T.M., Clark, S.K., Zhu, X.K., Wang, X.L., 2014. Selenium redox cycling during weathering of Se-rich shales: A selenium isotope study. Geochim. Cosmochim. Acta 126, 228–249.
Zingaro, R.A., Dufner, D.C., Murphy, A.P., Moody, C.D., 1997. Reduction of oxoselenium anions by iron (II) hydroxide. Environ. Int. 23, 299–304.